Pulp Screen Plugging Characteristics

Parsa Aryanpour [a,*] Robert W. Gooding [a,b] and James A. Olson [a]

Aperture plugging is a phenomenon that limits both the capacity and efficiency of pulp screens, which are critical components of the papermaking process. An understanding of how plugs are created and how they can be avoided can enhance the manufacture of paper products, providing energy savings, increased productivity, improved product quality, and higher levels of paper recycling. This work considers the creation and dispersion of plugs in a small, industrial screen. Flow resistance provides a means of assessing the presence of plugs and their evolution through creation and dispersion. A structured means of plug dispersion was formulated, from which floc strength could be inferred. These novel measurements provide insight not only into the factors that control plug creation, but into their character. Long-fiber (softwood) plugs were found to form and consolidate quickly and to achieve high strength. Their low porosity limited flow through the slot soon after creation. Short-fiber (hardwood) plugs formed more slowly, and they were more porous and weaker.

DOI: 10.15376/biores.20.1.1820-1837

Keywords: Pulp screening; Aperture plugging; Plug strength; Plugging mechanism

*Contact information: a: Department of Mechanical Engineering, The University of British Columbia, 6250 Applied Science Lane, Vancouver, BC, Canada, V6T 1Z4; b: Aikawa Fiber Technologies, 5890 Monkland Avenue, Suite 400, Montreal, QC, Canada, H4A 1G2; *Corresponding author: parsaary@mail.ubc.ca*

INTRODUCTION

Screening Process

A pulp screen is a piece of industrial process equipment that removes oversize contaminants from pulp suspensions, or in some other applications segregates fibers based on their lengths, *i.e.*, fractionation (Olson 1996). The principle performance components within a pulp screen are a screen cylinder, which has apertures in the form of holes or slots, and a rotor.

In a typical screening process, a suspension of water and pulp fibers enters the screening zone, *i.e.*, the annular space between the cylinder and the rotor within, axially through the feed end. The suspension is bifurcated into: 1) an accept stream with the desirable pulp fibers flowing radially outward through the cylinder apertures, and 2) a reject stream with oversize contaminants flowing axially toward the opposing end of the cylinder. The rotor fluidizes the pulp suspension, accelerates the suspension to a high circumferential velocity, and creates suction pulses. The pulses intermittently backflush oversized contaminants, pulp accumulations, and any other material from the slots and thus prevent cylinder plugging, which would otherwise halt production and incur significant production downtime.

Pulp Fibers and Rheology

A suspension of pulp fibers will have variations in fiber concentration on the scale of a fiber length due to fiber flocculation. The flocs themselves may be a factor in the creation of plugs. Crowding factor (N) is a parameter that helps to characterize fiber-fiber contact and the degree of flocculation in water suspensions (Kerekes and Schell 1992), and is described below,

$$N \approx \frac{5 C_m L_w^2}{\omega} \quad (1)$$

where C_m (%) is mass-based pulp consistency, L_w (m) is length-weighted average fiber length, and ω (kg/m) is fiber coarseness. Certain values of N have been associated with regimes where critical behavior changes occur in pulp suspensions (Mason 1950; Soszynski and Kerekes 1988; Kerekes and Schell 1992; Martinez *et al.* 2001; Celzard *et al.* 2009). Notably, $N \approx 60$ is known as the "rigidity threshold" (Celzard *et al.* 2009), which is the point at which each fiber contacts, on average, three other fibers. This is an important value because fibers are restrained by three-point contact. Due to eddies and other flow structures, fibers in such a suspension bend elastically and become interlocked due to the mechanical strength added to the network by the normal forces, creating friction at each contact point (Derakhshandeh *et al.* 2011). Below a crowding factor of 60, fiber flocs that form during shear flow are considered loose while above this value, flocs assume significant mechanical strength. Floc diameter is of the order of the fiber length, but the exact size and strength of flocs are dependent on the flow conditions. Decaying turbulence, such as is found in the wakes of pumps and mixers, are favorable conditions for floc formation, and thus an increase in fiber suspension heterogeneity (Kerekes 1983; Derakhshandeh *et al.* 2011). Other forces, such as those from hooking of curved fibers or from chemical flocculants, may add mechanical strength to the fiber network (Kerekes *et al.* 1985).

Screen Plugging Fundamentals

Fluid-driven plugging, as is the case in pulp screening, has been less researched than plugging in gravity-driven flows. Though they share similarities, fluid-driven models allow for additional insight into the effects of particle concentration, velocity, fluid-particle interaction, and hydrodynamic effects (Guariguata *et al.* 2012). While some studies (To *et al.* 2001; Dai and Grace 2010; Guariguata *et al.* 2012; Villalba *et al.* 2023) describe plugging mechanisms in idealized flow conditions, they were conducted under conditions that were far removed from industrial pulp screening: at velocities up to three orders of magnitude lower than pulp screening, without the pulsatile action of the rotor, with relatively stiff fibers, or without the high-consistencies that are intrinsic to industrial pulp screen operation.

Martinez *et al.* proposed a force balance model of fiber flocs lodged within screen slots, *i.e.* a "cork-in-a-bottle" mechanism (Martinez *et al.* 1999). They claimed that there are three forces on a given floc that contribute to this balance, namely a hydrodynamic force (F_H) due to the pressure differential across the screen plate, pulsation force (F_P) due to the pressure pulse from the rotor, and frictional force (F_F) from the slot walls. It was claimed that F_H tends to push the floc through the slot to the accept side of the screen, whereas F_P pulls the floc back to the feed side and F_F resists motion in either direction. A static equilibrium among the three forces defines the stage at which no net force acts to dislodge the floc.

Salem investigated the effects of pulp type, rotor tip speed (V_t), and the average speed through the slots (V_s) on pulp screen capacity and plugging (Salem 2013, 2014). He used a Beloit MR8 pulp screen equipped with a rotor that had two NACA 0015 foils with a 40-mm chord length and 6° angle-of-attack. The associated screen cylinder was a wedge-wire design with a contour height of 0.9 mm, wire width of 3.2 mm, and slot width of 0.15 mm (Salem 2013, 2014). Salem plotted the V_t needed to induce screen failure (*i.e.*, V_{tp}) at various V_s, feed consistencies, and blends of softwood and hardwood fibers. He found nearly parallel lines of increasing V_{tp} for increasing V_s for each consistency. A directly proportional relationship was established between consistency and V_{tp} by extrapolating the lines for each consistency and finding the intercepts on the V_t axis. The nearly-zero intercept suggested, as expected, that for a 0% fiber concentration (*i.e.*, water) a V_t of 0 m/s would be sufficient to prevent screen plugging.

Objective and Overall Approach

The aim of this work was to understand aperture plugs, the plugging mechanism, and plugging dynamics by creating plugs, allowing them to consolidate, and then eliminating them in a representative flow environment. A parameter to quantify the strength and character of the plugs is proposed. These insights serve the larger goal of developing screen hardware designs and operating practices that increase the capacity and reliability of screen equipment.

Through combining the observations from Martinez *et al.*'s work (1999), Salem's study (2013), and Kerekes and Schell's work (1992) regarding fiber crowding and flocculation, one could hypothesize that reduced V_t reduces the degree of pulp fluidization, along with the frequency and strength of backflushing pulsations, and some of the resulting fiber flocs might be small enough to pass through the slot entry, but large enough to stagnate at the narrowest slot region, *i.e.*, the "throat", creating incipient plugs. This would start as a momentary phenomenon and one of the following scenarios would happen: 1) the rotor would backflush the pulp accumulation, or 2) the pressure differential across the aperture would compress or disrupt the accumulation so that the fibers would pass to the accept stream, or 3) the accumulation would dewater and become immobilized in the slot. Decreasing V_t or increasing V_s could be hypothesized to increase the frequency and severity of the third scenario leading to incipient plugs, plug consolidation, and ultimately a fully-plugged slot.

EXPERIMENTAL METHODS

MR8 Pulp Screen and Flow Loop

A Beloit MR8 laboratory pulp screen (Fig. 1) at the UBC Pulp and Paper Centre was used to conduct the experiments. This screen model has a cylinder that is 203 mm in diameter and 254 mm in length. The cylinder was an AFT MacroFlow™ wedge-wire cylinder with a 0.15-mm-wide slot, 3.2-mm-wide wire, and 1.2-mm contour height. A variable frequency drive (VFD) controls the speed of the AFT EP™ rotor inside the cylinder. Two foils (60 mm chord length) are attached to the rotor and set at 0° angle-of-attack with 2.6 mm gap to the screen cylinder.

For a particular trial, either water or a pulp suspension was pumped from a 300-L tank to the screen by a VFD-equipped open-impeller pump and then returned through the

accept and reject lines to the tank so that the screen loop operated in continuous recirculation. Ball valves on the accept and reject lines were controlled using LabView software (National Instruments, version 8.6, Austin, TX, USA). Magnetic flow meters and flush-diaphragm pressure transmitters (models given in Table 2) monitored the flow rates and pressures on the feed, accept, and reject lines. Flow and pressure data and the rotational speed of the rotor were collected at 1000 Hz and saved using LabView.

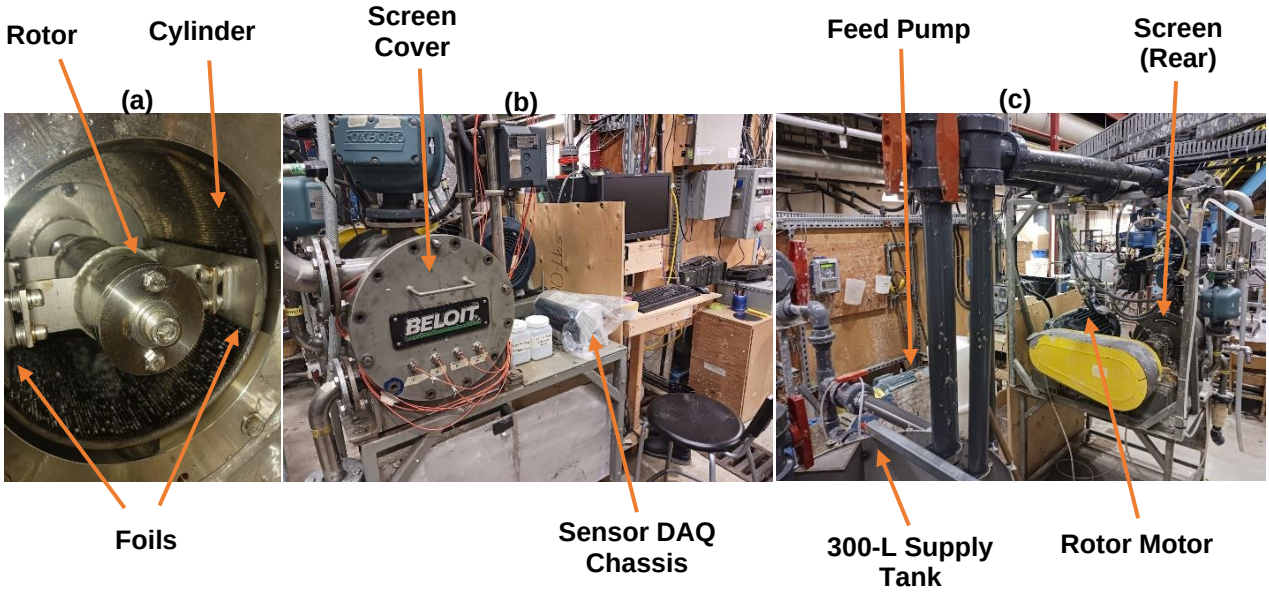

Fig. 1. (a): Two AFT EP foils inside the MR8 pulp screen (with the left foil only partly visible); (b): Screen cover; (c): Pilot plant testing apparatus

Pulp

Two pulps were tested: A northern bleached softwood kraft (NBSK) pulp produced from a spruce, pine, and fir furnish from the interior of British Columbia, and a bleached hardwood kraft (BHK) pulp produced from an aspen furnish in Alberta. Bleached market pulps were selected due to their wide availability and stability, allowing for more reliable experimentation over time and facilitating reproducibility of the study. Fiber properties measured using the Fiber Quality Analyzer (Table 1) were similar to values in the literature (Reeves *et al.* 1993; Gharehkhani *et al.* 2015; de Assis *et al.* 2019).

Table 1. Physical Properties of Pulp Fibers

Pulp Type	L_w (mm)	Coarseness (kg/m)	Diameter (μm)
Softwood	2.50	13.4×10^{-8}	28.6
Hardwood	0.78	10.3×10^{-8}	21.9

The pulp suspension for a given trial was prepared by reslushing dry pulp sheets in the supply tank that was typically filled to 250 L. The tank was equipped with a VFD-controlled mixer. The reslushing operation was performed with the mixer, without the pump in operation, until no flakes were apparent in a collected sample. The returning flows to the tank provided considerable agitation, but to be certain that there would be no stratification, the mixer was run continuously during all trials. The temperature of the

suspension was 15 °C and would rise by approximately 10 °C per hour of continuous operation. A new pulp suspension was prepared for each trial to minimize the accumulated effect of changes in pulp characteristics during recirculation for the ~0.5 h of operation of a typical trial.

Trial Protocol

General

At the start of a trial, the pulp or water was prepared as discussed previously. The screen rotor was started at the specified initial V_t. The pump was started with the accept valve closed and the reject valve fully open. The accept valve was then gradually opened until the target initial V_s was reached, and then the reject valve was gradually closed until the volumetric reject ratio (*i.e.*, R_v, the reject flow divided by the feed flow) reached a value of 17%, which is a typical industrial value. At this point, the sample valves and debris trap valve would be opened and closed momentarily to allow trapped air to escape, which might otherwise skew sensor readings. The feed pump VFD was set to produce a feed pressure of ~125 kPa. This provided a suitable range of V_s (~0.7 m/s to 2.4 m/s) at the target volumetric reject ratio. Moreover, increased post-plugging feed and reject line pressures would still stay below the safety limit (~250 kPa) at these settings.

Plugging trial protocol

Plugging was achieved using two approaches: decreasing V_t or increasing V_s while maintaining the other speed constant. For the first method ("V_t triggering"), performed at a range of consistencies, V_s was kept at a constant value of 1.5 m/s while decreasing V_t from 23 m/s to the point of plugging (V_{tp}) by increments of 1 rpm (~ 0.01 m/s). For the second method ("V_s triggering"), performed at 1.5% feed consistency (C_f), three V_t values were chosen based on the results of the V_t study: one below and two above the V_{tp}. The V_t was kept constant while V_s was increased from 0.7 m/s to the plugging value (V_{sp}) by opening the accept valve in 1% increments while opening the reject valve accordingly to maintain a constant R_v.

When plugging occurred, the valve positions and V_t were kept constant until the end of the test when steady-state flow conditions were achieved through the screen (*i.e.*, until noticing pressure and flow stabilization monitored on the live LabView plots). Recordings were then stopped and the plugging trial was deemed to have ended. The pump, rotor, and tank mixer were then stopped.

Unplugging trial protocol

Tests to unplug a cylinder were performed for each trial. From an industrial perspective, there is an interest in exploring possible ways to restore the screen to normal operation. Moreover, and perhaps more importantly, unplugging gives insight into the character of the plug itself, the factors that lock the plug into the slot, and the mechanical integrity of the plug. A standardized unplugging test was developed and used on each plugged cylinder. To prepare for an unplugging test, it was important to ensure that a plugged cylinder was not touched or removed from its MR8 enclosure so as to not risk changing the plug character from the end of the plugging test to the beginning of the unplugging test. Then, the flow loop was purged of the pulp suspension used for the plugging test and the feed tank was filled with 250 L of water. This was done to minimize the influence of pulp consistency on the unplugging action, though fibers from the plugged

cylinder would get reintroduced into the circulation as the cylinder became unplugged. The valve positions were then set to provide 1.5 m/s V_s at 17% R_v once the screen was unplugged (*i.e.*, 56% open for the accept valve, 58% open for the reject valve). V_t was initialized at 3 m/s and increased by 1 rpm (~0.01 m/s) per second until the cylinder was cleared of pulp, as signified by an audible rush of flow through the accept line, and the accept flow reaching 1.5 m/s at 17% R_v.

After performing unplugging tests, the rotor was stopped, the tank emptied and the cylinder was removed from the MR8 housing. Prior to starting the next trial, the cylinder was pressure-washed.

Uncertainty Analysis and Repeatability

Values of V_t and V_s at which the screen plugged (V_{tp}, V_{sp}) or unplugged (V_{tu}, V_{su}) were used as an overall measure of repeatability for the tests. Two-to-five tests were performed for each condition and error bars were produced based on a 95% confidence interval using the t distribution. For all other results, data from the most recent set of trials were used for calculations and the associated uncertainty figures were derived using the formula for uncertainty propagation, where the uncertainty Δz of a calculated value z is a function of values x and y and their uncertainties Δx and Δy as shown below. This was shown for one or two representative tests in the plots.

$$z = f(x, y) \tag{2}$$

$$\Delta z = \sqrt{\left(\frac{\partial f}{\partial x}\right)^2 (\Delta x)^2 + \left(\frac{\partial f}{\partial y}\right)^2 (\Delta y)^2} \tag{3}$$

Table 2. Sensor Accuracy of Devices Used in Testing Apparatus

Sensor and Location	Manufacturer	Model	Accuracy
Feed/Accept/Reject Pressure	WIKA (Klingenberg, Bavaria, Germany)	S-11	2 kPa
Accept/Reject Flow Rate	Foxboro (Foxborough, MA, USA)	IMT25 8300 series Flowtube with IMT25 Transmitter	0.25% of reading

RESULTS AND DISCUSSION

Cylinder Plugging

The plugging and unplugging points for the V_t and V_s triggering methods are shown in Fig. 2 and 3, respectively. The points in these figures represent the values of V_{tp} and V_{sp}, or V_{tu} and V_{su} that triggered screen plugging and unplugging.

The results in Fig. 2 show that increased C_f required a higher V_t to maintain an operational screen. Furthermore, SW pulp suspensions required a higher V_t to maintain an operational screen than HW pulp suspensions. These findings are consistent with Salem *et al.*'s findings (2013, 2014), and the crowding factor can be used to understand them. Higher consistencies and increased fiber length both increased the crowding factor, thus increasing fiber-fiber interactions and the degree and scale of flocculation. A higher crowding factor in turn, required increased V_t to create sufficient turbulence and fluidization to avoid

plugging. The SW pulp had considerably longer fibers compared to the HW pulp and only slightly higher coarseness, leading to much higher crowding factor for a given consistency. However the crowding factor clearly was not the only factor in plugging, as can be seen in Fig. 4, which is a replotting of Fig. 2 with crowding factor replacing consistency on the x-axis. The SW plugging datapoints did not follow those of HW plugging. Indeed, the high level of turbulence and complexities of fiber deposition could well mean that crowding factor and floc mechanics are at play. The unplugging datapoints of SW, though, seem to be following those of HW, as will be discussed in the unplugging section below. This would be a stronger conclusion with the addition of overlapping data points (*i.e.* some higher consistency HW points and some lower consistency SW points).

The results in Fig. 3 show that the minimum V_t needed to maintain an operational screen was directly proportional to V_s , consistent with Salem and co-authors (Salem 2013; Salem *et al.* 2014). As V_s increases, V_t must increase to induce sufficient fluidization and backflushing to counteract the increased overcrowding of the fibers at the slot entry.

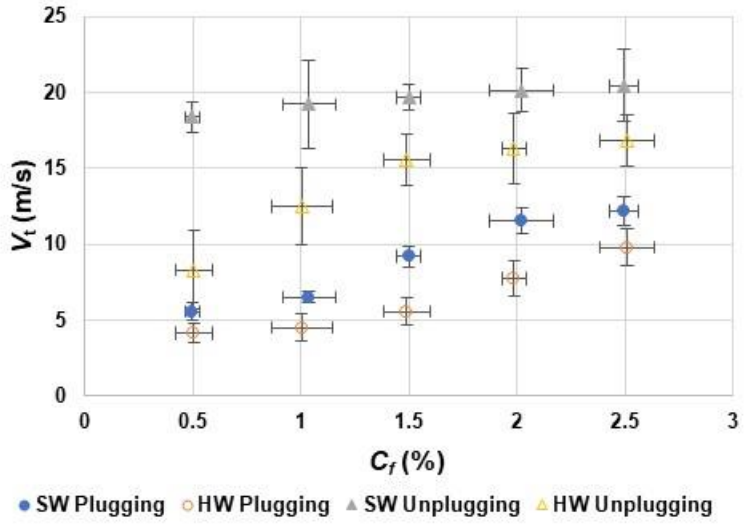

Fig. 2. Plugging (V_{tp}) and unplugging (V_{tu}) points using V_t plugging trigger (V_s = 1.5 m/s)

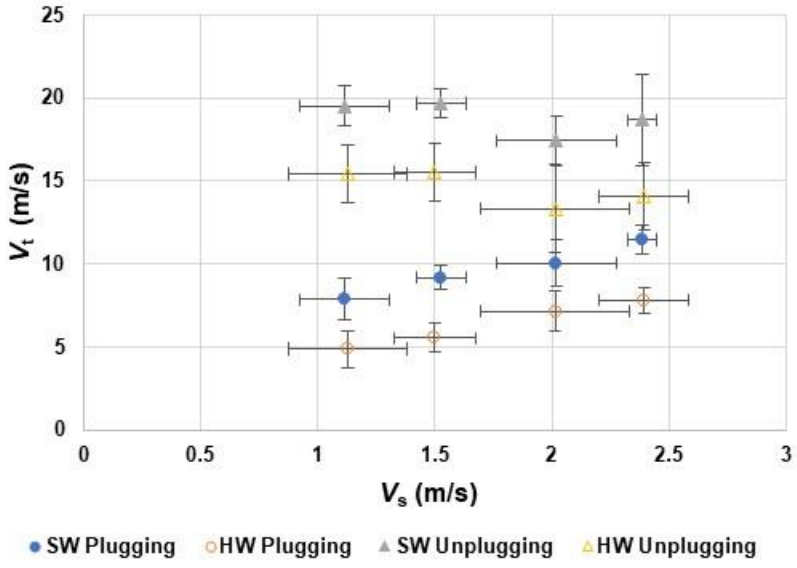

Fig. 3. Plugging (V_{sp}) and unplugging (V_{su}) points using V_s plugging trigger at 1.5% C_f

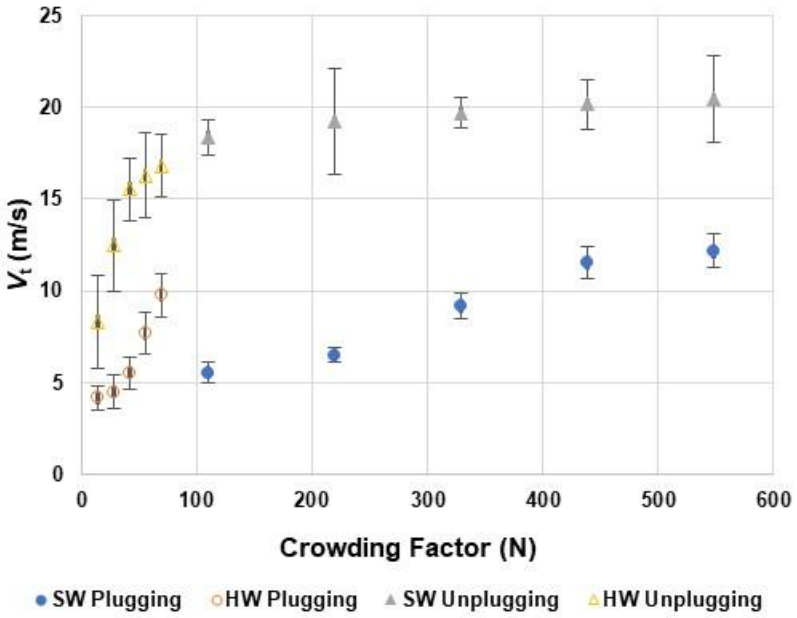

Fig. 4. Plugging (V_{tp}) and unplugging (V_{tu}) points using V_t plugging trigger (V_s ~ 1.5 m/s)

Cylinder Unplugging

Results from the unplugging tests are juxtaposed with screen plugging results in Figs. 2 and 3. The V_s or C_f at which a plug is created (x value) was combined with the V_{tu} required to clear the cylinder slots of pulp (y value). The results demonstrated an underlying hysteresis effect, also shown in recent literature (Villalba *et al.* 2024), whereby the V_t required to unplug and clear the slots (*i.e.*, V_{tu}) was much higher than the V_t that caused the slots to plug (*i.e.*, V_{tp}).

A possible explanation for the hysteresis goes back to one proposed mechanism for plug creation: Fiber accumulations that form in the slots may, under the appropriate conditions, become incipient plugs that are formed and dispersed. Further adverse conditions lead to plug creation. More specifically, the plug would then pass into a consolidation phase, which occurs as the plug is dewatered due to the pressure difference across the screen cylinder and the high-frequency rotor pulsations. The plugs may become further strengthened in a consolidation phase as they admit more fibers into their networks due to the constant feed supply. The factors that initially acted to counter plug creation (*i.e.*, the turbulence and the suction pulse of the foils) remain and may intensify plugging after the triggering event. As long as the parameters that led to the creation of the plug continue, the plug will remain. Removing the plugs in the unplugging process then takes a higher V_t due to this post-plugging consolidation of the plugs, hence the hysteresis. In considering the model of Martinez *et al.* (1999), one thus adds the complexity of the plug changing character after plugging.

As shown in Fig. 2, plugs made with SW pulps required a higher V_{tu} to unplug compared to plugs made with HW pulps at equivalent consistencies. It may be that the longer SW fibers form floc networks that were more consolidated and tightly-wound within the slot walls. As will be shown below, SW pulps created plugs that allowed less fluid travel through the plug interstices and therefore, it is reasonable that larger forces would be required to remove SW plugs. An interesting correlation related to unplugging appears in Fig. 4, where the strength of the developed plug is related to crowding factor and thus

flocculation levels of the suspension used to create the plug. The required V_{tu} increased sharply in the lower crowding factor region associated with HW pulps (N < 100) and then plateaued in the upper region for SW (N = 100 - 550). V_{tu} was relatively independent of the consistency for SW plugs, varying by ~10% across the range of consistencies of 0.5 to 2.5%. However, the V_{tu} for HW plugs showed greater sensitivity to concentration, especially in the 0.5 to 1.5% region. The SW observation can be explained by the possibility that the length of the fibers overshadows the effect of consistency for creating plug consolidation. For the HW pulps, it may be that because the fibers are shorter, consistency becomes a noticeable factor for plug consolidation until a value of ~1.5%, after which its effect diminishes, and the fiber network reaches a plateau of saturation (*i.e.*, no more fibers being able to infiltrate the compact network) in the slots, as dictated by crowding factor. It will be shown below that these observations are supported by measurements of the pressure drop coefficient K.

The influence of varying V_s was found to be relatively minimal on unplugging, as can be seen in Fig. 3. Therefore, the following discussion will be mainly in terms of the V_t trigger method. There is only a slightly downward overall trend in V_{su} for plugs made at higher V_s and therefore a higher constant V_t. It may be that post-plugging, the higher V_t prevented a larger number of fibers from integrating into the plugs and further consolidating them, resulting in plugs that are easier to unplug, *i.e.*, needing a lower unplugging V_{tu}.

Plugging Dynamics and *K*

Pre-plugging flow

The onset of plugging generally occurs suddenly, *i.e.*, within seconds, regardless of the triggering method. Novel methods, such as described by Aryanpour and co-authors (Aryanpour 2024; Aryanpour *et al.* 2024), have enabled the detection of incipient plugging, which is a precursor of plugging, but these have not been applied industrially. For a typical V_t triggering trial, the feed-to-accept pressure differential (ΔP_{fa}) and V_s stay constant at around 14 kPa and 1.5 m/s (*i.e.*, the same values as the water benchmark) as V_t is decreased, up until a rise in ΔP_{fa} and decline in V_s, signifying the plugging, as was described in Estevez-Reyes (1995).

Post-plugging flow

Noticeable accept flow remains from the beginning of plugging up to the point of plug consolidation and flow/pressure stabilization. Pressure drop coefficient (K), which is also termed hydraulic resistance, can be used to describe the ease of fluid travel through the plug. It requires fluid density as an input, which previous works (Gooding 1996; Martinez *et al.* 1999) have approximated as that of water for low-consistency screening, which is the subject of the current work,

$$K = \frac{\Delta P_{fa}}{0.5 \rho V_s^2} \quad (4)$$

$$\Delta P_{fa} = P_{feed} - P_{accept}\ [Pa] \quad (5)$$

where ρ is the fluid density (kg/m^3) and V_s is the slot speed (m/s).

The value of K rises during plugging, signifying an increase in flow resistance across the screen cylinder due to the consolidation of plugs within the screen slots. Post-

plugging results are shown in the following figures over time, with the start of plugging set at time zero. The key observations are as follows:

- Figures 5 and 6 show the rapid ΔP_{fa} increase and V_s decrease at the beginning of plug formation, followed by gradual stabilization over time, presumably while the plugs consolidate.
- Both ΔP_{fa} (Fig. 5) and V_s (Fig. 6) show higher flow resistance through the screen for longer fibers and higher C_f, *i.e.*, higher N. As shown with the higher K values for these pulps in Figs. 7 and 8, the fiber plugs within the slots are assumed to be denser with higher network strength (Kerekes and Schell 1992) and smaller interstices.
- For all C_f in these tests, SW pulps created plugs where V_s decreased to less than 0.1 m/s at steady state (*i.e.*, ~3% of the initial V_s). The time required to reach this steady-state value is less than 100 s for SW C_f of 1.5% and greater, in contrast to over 1000 s for 0.5% SW C_f.
- The HW pulp suspensions required longer, on the order of 500 s, to approach a steady state V_s. More importantly, even for 2.5% C_f, the steady-state V_s was ~0.6 m/s, equating to ~40% of the initial accept flow. It may be that this steady-state value represents a balance at which rotor pulses prevent more fibers from integrating into the plugs for further consolidation. For the smaller HW fibers, there are still large spaces in the plug network when this balance is achieved, thereby allowing considerable flow. For SW pulps, the plug's fiber network has much smaller openings in the consolidated pulp plugs. The notion that smaller HW fibers create a more porous plug is counter-intuitive but it may be explained by the higher degree of compression that occurs when the relatively large SW flocs are compressed into the slot.
- Values of K (Fig. 7) for SW fibers are two orders of magnitude larger than for the HW pulps, as shown in Fig. 8. Division by the square of a V_s value close to zero for SW pulps results in large K and the unsteadiness of the lines is the result of small variations in these very low V_s. A similar curve form is seen for the consistencies of 1.5% and above. The order of the curves is generally that higher consistencies give higher K, but the order is not followed for 2.0% HW, reflecting the noise in calculating K.
- Figure 9 shows that at steady state (*i.e.* stable V_s and ΔP_{fa}) after plugging, HW accept consistency (C_a) did not change much from the C_a just before plugging. This is the case while ΔP_{fa} increased dramatically and V_s only reduced by about half. There are two possibilities for what could have happened: First, it could be that HW plugs, which are documented to be substantially weaker than SW plugs, were "dynamic plugs" that were continually shedding and accumulating fibers. Alternatively, it could be that the slot was not completely plugged along its length. In this model, plugs may have been static, but the accept consistency did not change because the static plugs only occupied part of the slot length. This would have been enough to restrict the flow and elicit the plugging signal (*i.e.*, a sharp increase in K), but the remaining accept flow passed through with no change in C_a. For SW plugs, V_s decreased by ~90% (*versus* ~50% for HW) and C_a decreased by almost half for 2.5% SW. While both the shedding and partial plugging models may still apply to SW plugs, the latter would seem less likely and would have to have occurred to a much lesser degree for the ≥ 1.5% C_f cases given the combination of very restricted V_s and sharper drop-off in C_a post-plugging.

The above observations are consistent with the previous discussions regarding plugging: Increased fiber length, higher C_f (*i.e.*, higher crowding factor), and lower V_t facilitate the creation of plugs and the resulting plugs are assumed to be more consolidated and thus more resistant to removal.

The main consideration when studying K during plugging trials is that the values do not express information solely on the plugs, but rather on the plugs interacting with the fluids that create them. It combines the properties of the plug (*e.g.*, permeability) with those of the working fluid (*e.g.*, consistency, dynamic viscosity).

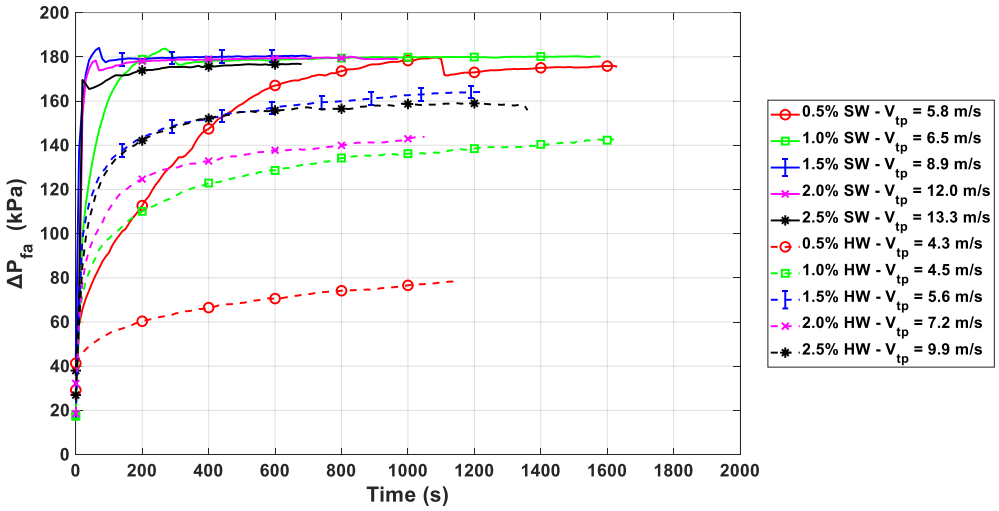

Fig. 5. ΔP_{fa} *versus* time elapsed after plugging by V_t trigger

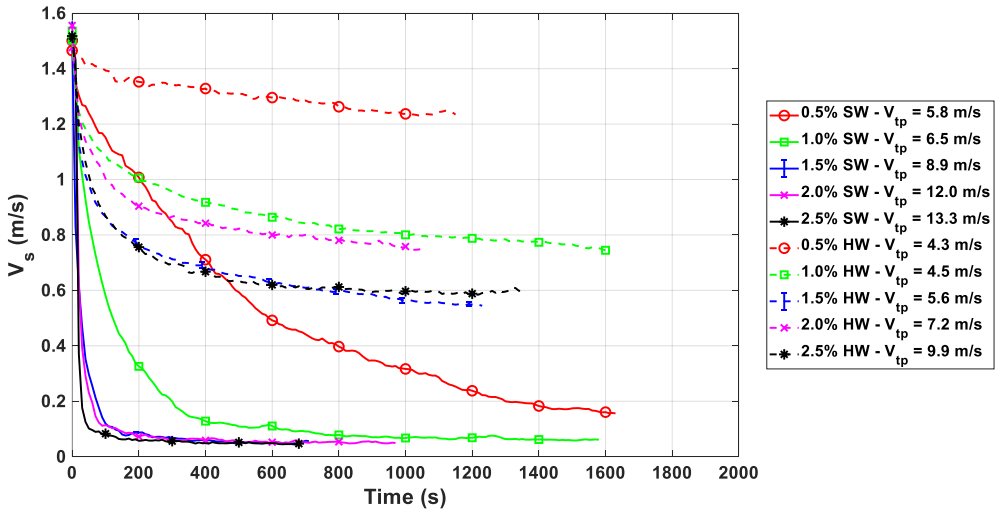

Fig. 6. V_s *versus* time elapsed after plugging by V_t trigger

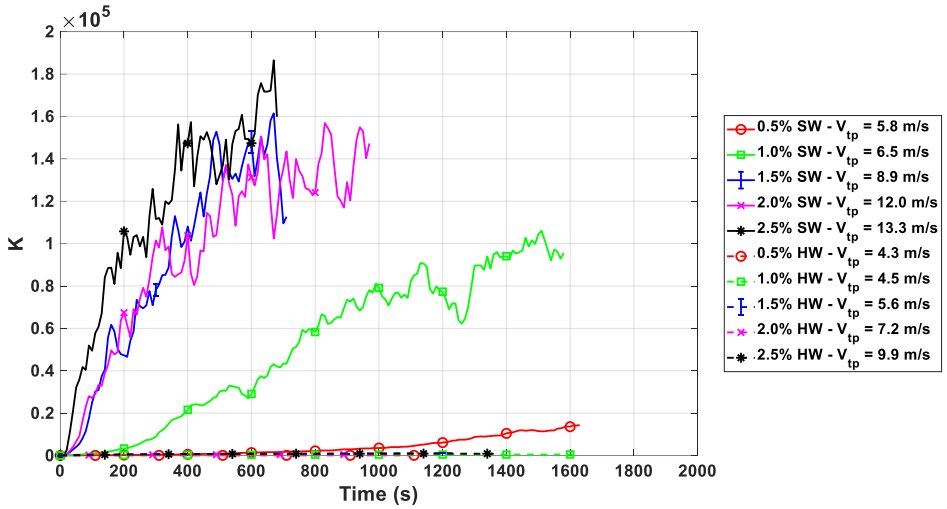

Fig. 7. K after plugging by V_t trigger (HW values are shown more clearly in Fig. 8)

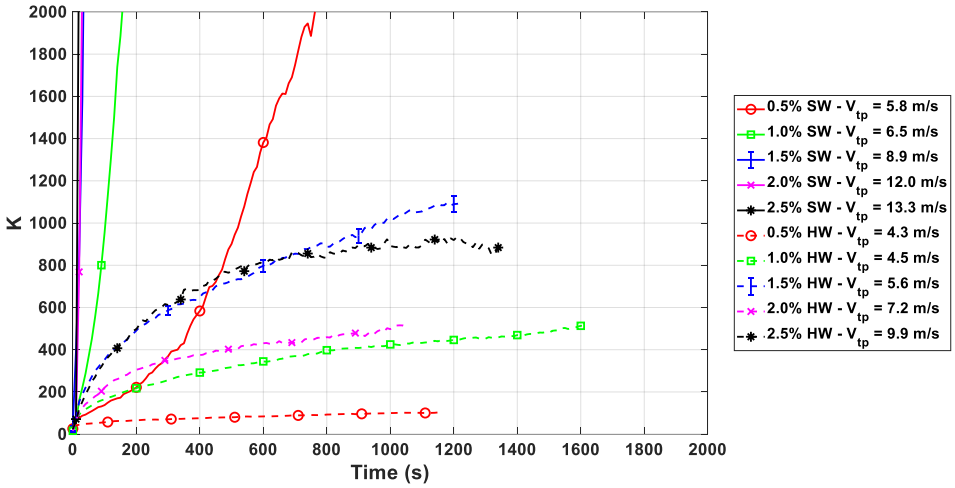

Fig. 8. K after plugging by V_t trigger

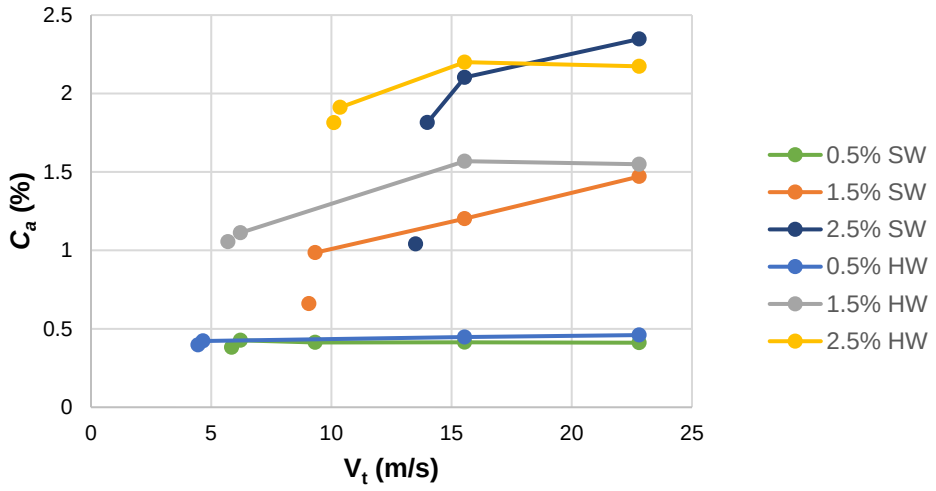

Fig. 9. C_a for V_t triggering: the second lowest V_t value is the last measurement captured prior to plugging; the lowest V_t value is the measurement captured after plugging steady state (*e.g.*, after ~700 s post-plugging, for 1.5% SW)

Unplugging Dynamics

Comparison to plugging

Unplugging behavior was found to be similar to plugging in that lower ΔP_{fa} (Fig. 10) and higher V_s (Fig. 11) resulted in lower K (Figs. 12 and 13) for screens plugged with lower C_f and shorter fibers. The plugs in the slots were likely less-highly consolidated for these conditions and created lower flow resistance for water during the unplugging phase. After unplugging, V_s returned to 1.5 m/s at 17% R_v, signifying the return to a clear cylinder.

Figure 14 is a schematic summary of the typical plugging and unplugging processes using K *versus* time. Specific values were from the 1.5% SW V_t trigger trial, but the concept is the same for all trials:

1) Normal Cylinder Operation: At this stage, $V_t > V_{tp}$ and $V_s < V_{sp}$. This stage can continue indefinitely as long as the two speed conditions are met. At speeds far from V_{tp} and V_{sp}, the pulp is fluidized and there is no persistent and substantial accumulation of fibers in the slot. As either or both values are approached, incipient plugging begins, whereby plugs are temporarily formed but lack the internal strength to persist within the cylinder slots for an extended period of time.

2) Triggering/Plug Creation: Cylinder plugging is triggered by either $V_t < V_{tp}$ or $V_s > V_{sp}$, or both. The main plugging mechanism likely happens in this stage, whereby a combination of factors, such as fiber length and concentration, are triggered to create persistent plugs within the slot that are strong enough to resist the hydrodynamic forces present at the slot. The trigger to plugging comprises increased slot throughput and/or decreased backflushing and agitation from the rotor. Pressure differential across the cylinder rises rapidly while V_s declines rapidly, leading to a sharp increase in K in the period after triggering.

3-4) Plug Consolidation: K then increases at a much slower rate than during the plug creation phase. It is hypothesized that the plug has entered a consolidation phase from Point 3 to 4, where plug density and strength are increased. The plug continues to consolidate until stable values of V_s and ΔP_{fa} are established. One important difference

between the HW and SW trials in this stage is that there is notable V_s after HW plugging (~0.5 to 1.3 m/s for the range of 0.5 to 2.5% C_f) *versus* much smaller values for SW plugging (~0.1 to 0.2 m/s for the range of 0.5 to 2.5% C_f). This leads to higher K values for SW, suggesting higher consolidation. The lower V_s for SW suggests that SW plugs are mostly static in nature and set permanently in the cylinder slots, whereas HW plugs could have a dynamic behavior of continuously receiving and shedding fibers. Alternatively, another possibility is that there may be gaps along the slot length for HW that are left unplugged. It may be that the rotor pulses in this regime dewater and strengthen the plug rather than serving their intended goal of plug removal.

4-5-6) Plug Destabilization: At Point 5, the feed pulp in the trial has been replaced with water. The sudden K decline relative to Point 4 is likely due to water travelling through the plugged slots with more ease than for the pulp suspension, as less viscous fluids permeate through a porous medium more easily (Muskat 1982). K then slowly decreases as V_t is increased at ~ 0.01 m/s^2. By applying increasingly strong and frequent pressure pulses, the plug is likely destabilized between Points 5 and 6, *i.e.*, weakened in integrity and/or means of restraint within the slot. The gradual rise in V_s during the plug destabilization regime that occurs for the SW trials and for HW trials with $C_f \geq 2.0\%$ (Fig. 11) suggests that plug-removal is occurring by erosion and a progressive de-structuring of the plug. One should note that the increase of V_t during the unplugging phase may take over 1500 s (*i.e.*, over 20 min) and the effect of a higher rotor speed is clearly not instantaneous.

6-7) Plug Elimination: This short period, typically < 100 s, sees a more rapid drop in K than the previous phase, despite the V_t rate-of-increase staying constant. It is assumed that during this phase, the weakened plug reaches a yielding period, breaks up, and is released from the slot. Thus, point 7 marks the end of the unplugging process whereby V_s returns to 1.5 m/s, signifying unplugging. The V_t at point 7 is designated as V_{tu} and a hysteresis effect is present whereby $V_{tu} > V_{tp}$ for the case that V_t triggering was employed to create the plug.

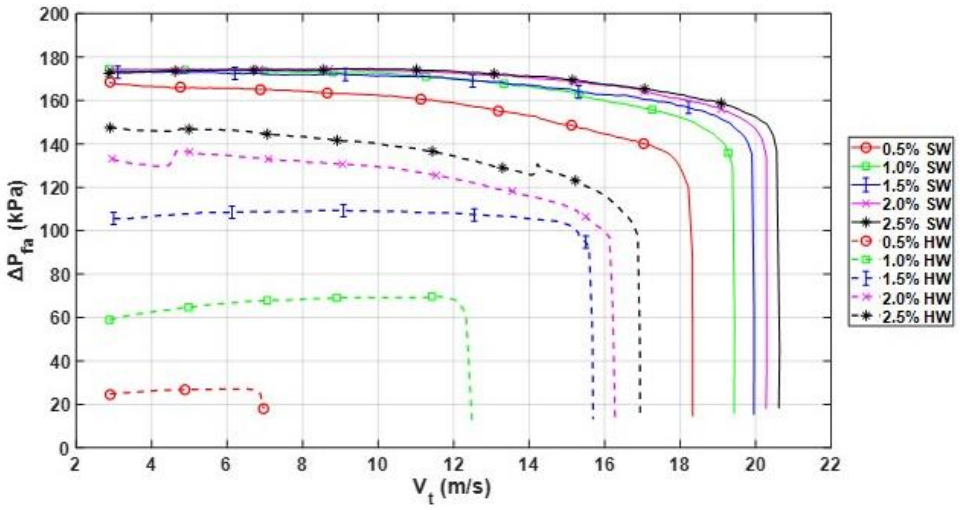

Fig. 10. ΔP_{fa} during unplugging for screens plugged with a V_t trigger

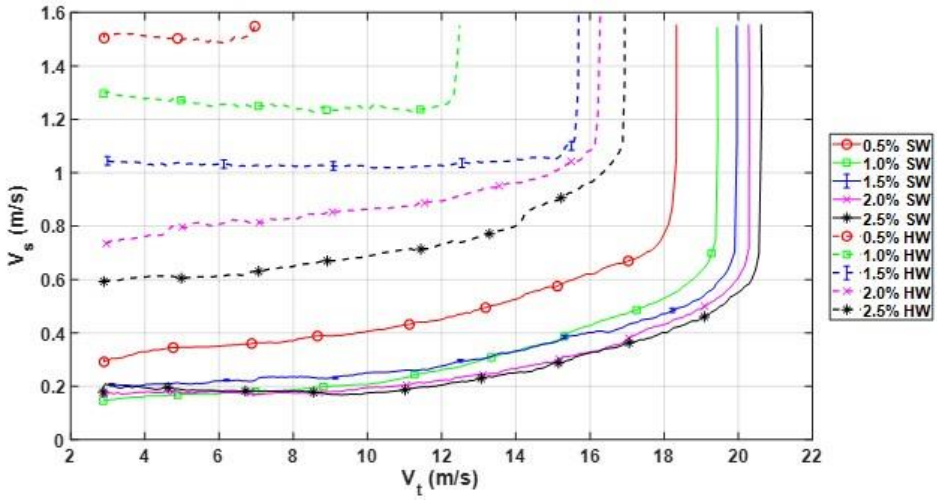

Fig. 11. V_s during unplugging for screens plugged with a V_t trigger

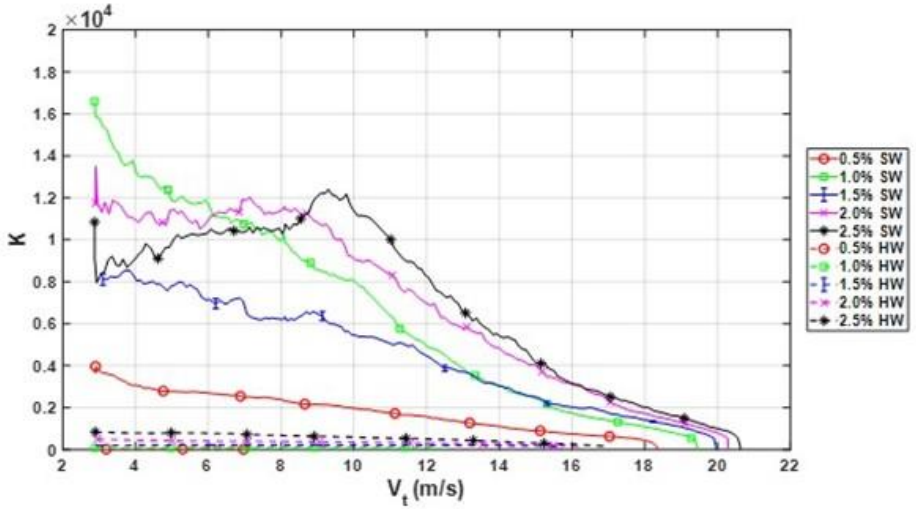

Fig. 12. *K* during unplugging for screens plugged with V_t trigger, HW values are shown in more detail in Fig. 13

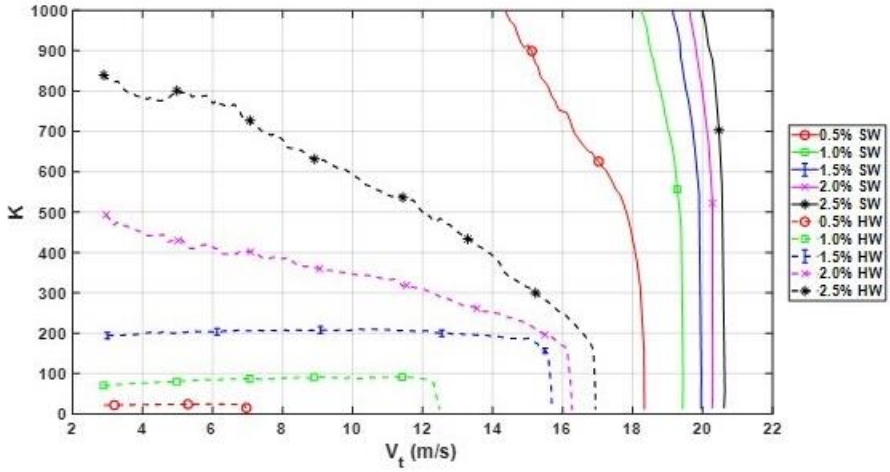

Fig. 13. *K* during unplugging for screens plugged with V_t trigger

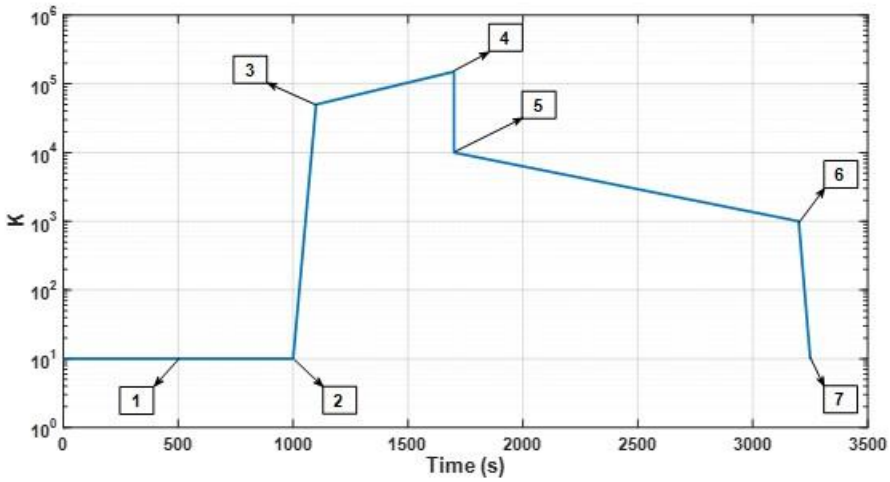

Fig. 14. Schematic stages of plugging and unplugging demonstrated using 1.5% SW V_t trigger example. The time = 0 point is set somewhat arbitrarily during a period of normal screen operation

CONCLUSIONS

1. Plug Strength: A novel means of assessing plug strength has been developed, which uses the unplugging rotor speed (V_{tu}) in a water-based environment. The strong role of Crowding Factor (N) was demonstrated by showing how a single curve can embrace the correlation of plug strength to N for both hardwood and softwood pulps. Stronger plugs were associated by higher feed consistencies and longer (softwood) fibres.
2. Plugging/Unplugging Regimes: The resistance of flow through the screen slots, characterized by K and measured by conventional industrial flow and pressure measurements, provides a means of characterizing plugging and identifying distinct regimes within the plugging and unplugging processes. Values of K can also be used to provide insight into plugging dynamics: For higher feed consistencies and longer (softwood) fibers, for example, K increases more quickly at the onset of plugging and achieves higher values.
3. Plug Character: The character of plugs may be inferred from the points where screen operation passes from one regime to another. For short (hardwood) fibers and at low feed consistencies, the plugs are weak and form slowly. There is substantial post-plugging flow through the screen cylinder and accept consistency does not decrease substantially. The opposite of these results is obtained at the other extreme for longer (softwood) fibers at high consistencies. Generally, a higher consistency for a given fiber type requires a higher rotor speed to avoid plugging or to unplug the cylinder.
4. Plug Complexity: The starting point for modelling fluid-driven plugging is a simple "cork-in-a-bottle" mechanism. The current study suggests a more complex model given the substantial plugging/unplugging hysteresis and the character of the aforementioned regime plot. While plugs are created quickly, the progressive increase of the accept flow during unplugging suggests that plug removal may follow a slow destabilizing and weakening of the plug and extraction of its fibers along or normal to the slot length.

The gradual reduction in K during unplugging instead of an instantaneous plug release-point indicates that erosion and progressive de-structuring underlies plug removal.

ACKNOWLEDGEMENTS

The financial and technical contributions of Natural Sciences and Engineering Research Council (NSERC), Aikawa Fiber Technologies, UBC Pulp and Paper Centre (PPC), UBC BioProducts Institute (BPI), Canfor Pulp Products, and Mercer International are gratefully acknowledged.

REFERENCES CITED

Aryanpour, P. (2024). *Plugging of Pulp Screen Apertures*, MASc Thesis, The University of British Columbia, BC, Canada. DOI: 10.14288/1.0441527

Aryanpour, P., Gooding, R., and Olson, J. (2024). "Detection of incipient pressure screen plugging," *BioResources* 20(1), 566-587. DOI: 10.15376/biores.20.1.566-587

Celzard, A., Fierro, V., and Kerekes, R. (2009). "Flocculation of cellulose fibres: New comparison of crowding factor with percolation and effective-medium theories," *Cellulose (London)* 16(6), 983-987. DOI: 10.1007/s10570-009-9314-0

Dai, J., and Grace, J. R. (2010). "Blockage of constrictions by particles in fluid–solid transport," *International Journal of Multiphase Flow* 36(1), 78-87. DOI: 10.1016/j.ijmultiphaseflow.2009.08.001

de Assis, T., Pawlak, J., Pal, L., Jameel, H., Venditti, R., Reisinger, L. W., Kavalew, D., and Gonzalez, R. W. (2019). "Comparison of wood and non-wood market pulps for tissue paper application," *Bioresources* 14(3), 6781-6810. DOI: 10.15376/biores.14.3.6781-6810

Derakhshandeh, B., Kerekes, R. J., Hatzikiriakos, S. G., and Bennington, C. P. J. (2011). "Rheology of pulp fibre suspensions: A critical review," *Chemical Engineering Science* 66(15), 3460-3470. DOI: 10.1016/j.ces.2011.04.017

Estévez Reyes, L. W. (1995). *Fault Detection on Pulp Pressure Screens*, Ph.D. Thesis, The University of British Columbia, Vancouver, BC, Canada. DOI: 10.14288/1.0065252

Gharehkhani, S., Sadeghinezhad, E., Kazi, S. N., Yarmand, H., Badarudin, A., Safaei, M. R., and Zubir, M. N. M. (2015). "Basic effects of pulp refining on fiber properties—A review," *Carbohydrate Polymers* 115, 785-803. DOI: 10.1016/j.carbpol.2014.08.047

Gooding, R. W. (1996). *Flow Resistance of Screen Plate Apertures*, Ph.D. Thesis, The University of British Columbia, Vancouver, BC, Canada. DOI: 10.14288/1.0058507

Guariguata, A., Pascall, M. A., Gilmer, M. W., Sum, A. K., Sloan, E. D., Koh, C. A., and Wu, D. T. (2012). "Jamming of particles in a two-dimensional fluid-driven flow," *Physical Review E* 86(6), article ID 061311. DOI: 10.1103/PhysRevE.86.061311

Heath Reeves, R., Plantikow, J. D., Smith, L. J., Philips Oriaran, T., Awofeso, A. O., and Worry, G. L. (1993). "Soft high strength tissue using long-low coarseness hesperaloe fibers," U. S. Patent No: US 5320710 A.

Kerekes, R. J. (1983). "Pulp flocculation in decaying turbulence: A literature review," *Journal of Pulp and Paper Science* 9(3), 86-91.

Kerekes, R., and Schell, C. J. (1992). "Characterization of fibre flocculation regimes by a crowding factor," *Journal of Pulp and Paper Science* 18, 32-38.

Kerekes, R. J., Soszyński, R. M., and Tam Doo, P. A. (1985). "The flocculation of pulp fibres," in: *Papermaking Raw Materials*: *Their Interaction with the Production Process and Their Effect on Paper Properties: Transactions of the 8th Fundamental Research Symposium*, Manchester, UK, pp. 265-310. DOI: 10.15376/frc.1985.1.265

Martinez, D., Buckley, K., Jivan, S., Lindstrom, A., Thiruvengadaswamy, R., Olson, J., Ruth, T., and Kerekes, R. (2001). "Characterizing the mobility of papermaking fibres during sedimentation," in: *The Science of Papermaking: Transactions of the 12th Fundamental Research symposium,* Manchester, UK, pp. 225-254. DOI: 10.15376/frc.2001.1.225

Martinez, D. M., Gooding, R. W., and Roberts, N. (1999). "A force balance model of pulp screen capacity," *Tappi J.* 82, 181-187.

Mason, S. G. (1950). "The motion of fibres in flowing fluids," *Pulp and Paper Canada Magazine* 51(5), 93-100.

Muskat, M. (1982). *The Flow of Homogeneous Fluids Through Porous Media*, International Human Resources Development Corporation Boston, Boston, MA, USA.

Olson, J. A. (1996). *The Effect of Fibre Length on Passage Through Narrow Apertures*, Ph.D. Dissertation, The University of British Columbia, Vancouver, BC, Canada. DOI: 10.14288/1.0058501

Salem, H. J. (2013). *Modeling the Maximum Capacity of a Pulp Pressure Screen*, Ph.D. Thesis, The University of British Columbia, Vancouver, BC, Canada. DOI: 10.14288/1.0103345

Salem, H. J., Gooding, R. W., Martinez, D. M., and Olson, J. A. (2014). "Experimental study of some factors affecting pulp screen capacity," *Nordic Pulp & Paper Research* 29(2), 218-224. DOI: 10.3183/npprj-2014-29-02-p218-224

Soszynski, R. M., and Kerekes, R. J. (1988). "Elastic interlocking of nylon fibers suspended in liquid: Part 1. Nature of cohesion among fibers," *Nordic Pulp & Paper Research* 3(4), 172-179. DOI: 10.3183/npprj-1988-03-04-p172-179

To, K., Lai, P. Y., and Pak, H. K. (2001). "Jamming of granular flow in a two-dimensional hopper," *Physical Review Letters* 86(1), 71-74. DOI: 10.1103/PhysRevLett.86.71

Villalba, M. E., Daneshi, M., and Martinez, D. M. (2023). "Characterizing jamming of dilute and semi-dilute fiber suspensions in a sudden contraction and a T-junction," *Physics of Fluids* 35(12), article ID 123339. DOI: 10.1063/5.0178933

Villalba, M. E., Olson, J. A., and Martinez, D. M. (2024). "Understanding the limits of a screening operation. Part 1: Characterization of screen plugging," *BioResources* 19(2), 2404-2416. DOI: 10.15376/biores.19.2.2404-2416

Article submitted: October 28, 2024; Peer review completed: December 9, 2024; Revised version received and accepted: December 17, 2024; Published: January 8, 2025.
DOI: 10.15376/biores.20.1.1820-1837